Fermi National Accelerator Laboratory

FERMILAB-Pub-82/98-THY
December 1982

# Four dimensional $CP^2$ on a Lattice

K.M.Bitar* and R.Raja

Fermi National Accelerator Laboratory

Batavia, Illinois 60510

## ABSTRACT

We investigate the phenomenon of dynamical generation of gauge interactions from $CP^{N-1}$ models in four dimensions. We do this for the $CP^2$ model on a lattice. The phase diagram of a model that interpolates between $CP^2$ and U(1) gauge theory on a lattice is first mapped out. The potential between static charges in various regions of this diagram is also measured. Contrary to hopes based on the large N behavior of similar models in two dimensions and on our phase diagram we find that the potentials generated by $CP^2$ do not bear any resemblance to those of U(1). They are rather similar to the Higgs phase of an abelian gauge theory in both phases displayed by $CP^2$ .

*On leave from the American University of Beirut, Lebanon.

Operated by Universities Research Association Inc. under contract with the United States Department of Energy

# I. INTRODUCTION

With the introduction[1] of the $CP^{(N-1)}$ models in two dimensions, it was recognized that aside from their property of having instanton solutions they also exhibit in the large N limit the interesting property of dynamical generation of gauge fields. Thus in effect a long range Coulomb force is generated from a current -current interaction. This is traced to the local gauge invariance that these models have built into their structure. This gauge invariance is expressed in terms of a (dependent) gauge field without a kinetic term added to the Lagrangian. However what one can show in the large N limit in two dimensions, where the model is renormalizable, is that an effective kinetic term is dynamically generated; the gauge field acquires a propagator of a dynamical nature through vacuum polarization processes.

This property is also shared, in an appropriate large N limit, by extensions of these models[2] which possess a similarly represented non-abelian gauge invariance ($HP^{N-1}$). Furthermore, extentions of both $CP^{N-1}$ and their non-abelian counterparts to supersymmetric versions is possible (3) and exhibit similar properties.

The extension of the supersymmetric version of these models to four dimensions was carried out by Cremmer and Scherk ( 4 ). They have also shown that supergravity theories incorporate such models in their structure and that it is through this mechanism that supergravity theories appear to exhibit "hidden" local gauge invariance symmetries.

The N=8 supergravity theory ( 5 ) in which all particles, except the graviton ,are thought to be composite relies heavily on the hope that the dynamical generation of (non-abelian and abelian ) gauge bosons will result out of the "hidden" local gauge invariance the theory has in a manner similar to the two dimensional $CP^{N-1}$ and $HP^{N-1}$ models. Thus in order to understand the validity of such theories one must answer the question of whether such a hope may be realized.

Since direct extensions of $CP^{N-1}$ and $HP^{N-1}$ to four dimensions leads to nonrenormalizable theories one cannot rely on the large N perturbative treatment of vacuum polarization graphs so useful in the two dimentional case. These graphs are highly divergent and hence cutoff dependent. Any attempt at removing this dependence via counter terms leads naturally to this term being $(F_{\mu\nu})^2$ where $F_{\mu\nu}$ is the field strength of the gauge field. This is tantamount to having started with a theory with this kinetic term built in. Thus one may not argue that the gauge bosons may be dynamically generated. In fact in this case one has elementary gauge fields interacting with the elementary scalar fields of $CP^{N-1}$ or $HP^{N-1}$ forming a Higgs type system. Probably the best that one can do with out a kinetic counter term in this case is to think of the four dimensional $CP^{N-1}$ and $HP^{N-1}$ models as leading to effective gauge theories valid at scales much smaller than the cutoff introduced.

With a kinetic term for the gauge fields one has essentially Higgs models with deep and narrow potentials for the scalar fields. Such models have been compared[6] at $d=4-\epsilon$ to $CP^{N-1}$ and $HP^{N-1}$ models in $d=2+\epsilon$. There is remarkable similarity of renormalization group functions for the two systems at $d=2+\epsilon$. It is this similarity that gives one hope that $CP^{N-1}$ and $HP^{N-1}$ may exist, though nonperturbatively, in four dimensions; indeed that the dynamical generation of gauge fields may be realized. Thus to understand this phenomenon ,at least partly, we turn to one of the few exploitable non-perturbative methods currently available; namely Monte Carlo simulations on a lattice.

We set up a simple $CP^2$ model on a four dimensional lattice and add on a kinetic term for the gauge field in the form of the Wilson[7] action for U(1). We then study the phase structure of this system and in particular calculate the potential between static charges as generated by $CP^2$ and the U(1) components separately and in combination. We find that $CP^2$ has a phase simply connected with the confining phase of U(1) (Fig.1). On the other hand $CP^2$ does not exhibit a phase similar to the Coulomb phase of U(1). This second phase is separated from it by a critical line and appears to be a continuation of the Higgs phase above this line; it also appears to exhibit a potential similar to that of this phase (Figs.2b,3b,4).

The following two sections present the lattice analysis we have carried out. We then end with a discussion and conclusions.

# II $CP^{N-1}$ ON A LATTICE

There are several formulations of the $CP^{N-1}$ models on a lattice. However, in order to exhibit the U(1) gauge invariance, we will use the direct transcription of the continuum model. The action reads

$$S_2 = -\beta_2 \sum_{i,\hat{\mu},\alpha} \left[ Z^*_\alpha(i)\, U_{i,\hat{\mu}}\, Z_\alpha(i+\hat{\mu}) + c\cdot c \right] \ldots\ldots (1)$$

Here i labels a lattice site, $\hat{\mu}$ a unit vector in one of the four euclidian directions and $\alpha = 1,\ldots\ldots,N$ labels the N complex scalar fields of $CP^{N-1}$. $Z_\alpha(i)$ and $U_{i,\hat{\mu}}$ label the complex scalar fields on the lattice sites and the usual gauge link variable respectively. The scalar fields on each site satisfy the constraint

$$\sum_{\alpha=1}^{N} Z^*_\alpha(i)\ Z_\alpha(i) = 1 \ \ldots\ldots (2)$$

In this work N=3 and we have $CP^2$. The scalar fields are then parametrized as follows

$$Z_\alpha(i) = P_\alpha(i)\ e^{i\,\Theta_\alpha(i)}$$

and the constraint of eq.(2) becomes

$$P_1^2(i) + P_2^2(i) + P_3^2(i) = 1$$

Thus the $P_\alpha(i)$ are the cartesian coordinates of a sphere of unit radius.

If we further define $\phi(i,\hat{\mu})$ as the U(1) gauge link angle we may write $S_2$ as

$$S_2 = -\beta_2 \sum_{i,\hat{\mu},\alpha} 2 P_\alpha(i)\, P_\alpha(i+\hat{\mu}) \quad \cos\left[\theta_\alpha(i) - \theta_\alpha(i+\hat{\mu}) + \phi(i,\hat{\mu})\right] \ldots (3)$$

If we further add a kinetic term to the gauge fields in the form of a Wilson action we have

$$S_1 = -\beta_1 \sum_{\text{PLAQUETTES}} 2 \quad \cos\left[\phi_P\right] \ldots . (4)$$

where $\phi_P$ is the usual plaquette angle given as the appropriate sum over the link angles $\phi(i,\hat{\mu})$.

The action $S=S_1+S_2$ is now that of a Higgs model on the lattice with N complex scalar fields in a narrow deep potential enforcing the constraint of eq(2). The pure $CP^{N-1}$ is the limit as $\beta_1 \to 0$ of S and the pure U(1) system is the limit $\beta_2 \to 0$ of S. Thus S interpolates between two systems whose properties we are to compare and contrast.

Furthermore in the limit $\beta_1 \to \infty$ the system S reduces to the O(2N) sigma model. For in this limit all gauge link angles are forced to zero and the action becomes

$$\lim_{\beta_1 \to \infty} S = S_2' = \sum_{i,\alpha,\hat{\mu}} -\beta_2' \left[ Z_\alpha^*(i)\, Z_\alpha(i+\hat{\mu}) + C \cdot C \right] \ldots (5)$$

which with constraint of eq.(2) is a lattice formulation of O(2N). This model is known to have a phase transition with calculable upper and lower bounds which for O(6) and our choice of $\beta_2'$ are

$$0.465 \geq \beta'_{2\,CR.} \geq 0.375$$

Thus our system S interpolates to this model as well and must reflect its critical structure.

The first step in our study is to see how, if at all, $CP^{N-1}$ simulates U(1) on the lattice; and in particular whether their phases interpolate smoothly among each other in the $\beta_1, \beta_2$ plane. Before discussing the Monte Carlo simulations let us now briefly discuss what one might expect on general grounds. Consider the $CP^{N-1}$ part of the action S . In the small $\beta_2$ limit (strong coupling) one may expand the Boltzman factor $e^{-S_2}$ and perform the integration over the scalar fields $Z_\alpha(i)$. The fundamental integral to be used is:

$$\sum_{\alpha=1}^{N} \int dZ^*_\alpha \, dZ_\alpha (Z^*_\gamma)^n (Z_\beta)^n \, \delta\Big(\sum_{k=1}^{N} Z^*_k Z_k - 1\Big) = \frac{2\pi n! \, \delta nm \, \delta\gamma\beta}{\Gamma(n+m)} \qquad (6)$$

The leading contribution that has gauge link variables present in a non-trivial way comes from the $(S_2)^4$ term where one obtains the product of four link factors $(\sum_\alpha Z^*_\alpha(i)\, U_{i,\hat\mu}\, Z_\alpha(i+\hat\mu)$ +c.c.) around an isolated plaquette. The result in terms of the gauge link variables is a Wilson action term with a coefficient $\sim (\frac{\beta_2}{6})^4$ for $CP^2$ . This term may be considered as the leading term in an expansion of a

Boltzman factor for a Wilson action in terms of these link variables. Thus at least for small $\beta_2$ one can generate from a $CP^2$ action the leading behavior of a Wilson U(1) gauge action.[10] This , on the lattice, is the corresponding behavior to the large N limit in two dimensions mentioned earlier. Thus two conclusions may be drawn from this observation. First, for pure $CP^{N-1}$ , one may expect for small $\beta_2$ a behavior similar to the confining region of U(1). Second for $\beta_1 \neq 0$ and $\beta_2 \rightarrow 0$ the U(1) action acquires an extra term with similar "relevant operators" and coefficient $O(\beta_2)^4$. Thus the behavior of the combined system will be the same as a pure U(1) with all values of $\beta_1$ shifted downwards. In particular the known phase transition at $\beta_{1CR.} \sim 1$ will now appear at a smaller value since one expects now to have $\beta_1 + O(\beta_2^4) = 1$. The important point here is that $CP^{N-1}$ contributes "relevant operators to the U(1) system. therefore we expect in the $\beta_1$ , $\beta_2$ plane a phase transition line emanating from $\beta_{1CR.} \sim 1$ and curving towards smaller $\beta_1$ as $\beta_2$ is increased above zero.

If $CP^{N-1}$ maintains this property for all $\beta_2$ then we would expect a phase transition along the $\beta_2$ axis and more importantly the phase transition line will continue to it approaching it from below as $\beta_1 \rightarrow 0$. This approach indicates that the U(1) "relevant operators" are also contributing to those of $CP^{N-1}$ even at large values of $\beta_2$ . We do not have a proof of this but present it as a possible signal to be looked for in the Monte Carlo simulation we perform. Further since in the $\beta_1 \rightarrow \infty$ limit one expects the system to reduce to O(2N) as explained above, one would expect a phase transition line to appear for large $\beta_1$ and within the limits known for the critical values of $\beta_2'$ of O(2N). If this line then terminates at a value of $\beta_1$ short of the line emanating from $\beta_{1CR.} \sim 1$ then the the Coulomb phase of U(1) may be smoothly connected with the small coupling phase of $CP^{N-1}$. Monte Carlo results for simple Higgs systems suggest otherwise however.[13] Since in the limit $\beta_2 \rightarrow \infty$ the model is trivial and the Higgs scalars carry unit charge one expects these two lines to meet. As we shall see the Monte Carlo simulation we perform supports this expectation.

To study the phase diagram in the $\beta_1$ , $\beta_2$ plane we set up the model on a $5^4$ lattice with periodic boundary conditions in all four directions. We measure the order parameters along thermal cycles and look for hysteresis curves. The location of the transition is determined by subtracting the heating curve from the cooling curve. Using all points that exhibit cooling-heating differences in the order parameter that is greater than 0.25 of the maximum such difference, we perform a weighted average. Each value of $\beta$ is given a weight proportional to the cooling-heating difference in the order parameter. The mean $\beta$ is then taken to be the phase transition point and the error in the mean is taken to be the uncertainty in the position of the transition.

The two order parameters are, first, the average energy per plaquette for gauge variables and, second, the average energy per link for scalar and gauge variables. We normally fix $\beta_1$ and/or $\beta_2$ and sweep in the other variable. We obtain , using the average energy per link, the results shown on Fig.1. A similar result is obtained using the plaquette energy but,except for values of $\beta_1$ near one , the error in the location of transitions is larger in this case. Clearly for $\beta_2$ =0 the only parameter available is the plaquette variable and we use it. We show in Fig.5 typical hysteresis curves at $\beta_1$ =0.5, and scanning in $\beta_2$ over the range zero to two. The differences used in locating the points of maximum separation are shown in Fig 6. Both order parameters are used. For U(1) we use the elements of Z(512).

As is clear from Fig.1 we have three distinct regions in the $\beta_1$ , $\beta_2$ plane separated by phase transition lines as anticipated above.

We see that the confining phase of U(1) connects smoothly with the strong coupling region of $CP^2$ . The phase transition curve joining the phase transition points along each axis has the correct curvature to indicate what we showed to be true for small $\beta_2$ ; namely that for all $\beta_2 \lesssim 0.82$, $CP^2$ and U(1) share some "relevant operators" and hence are expected to have similar behavior in that region.

The Coulomb phase of U(1) is clearly separated from the Higgs phase of the system which in turn connects smoothly with the region $\beta_2 \geq 0.82$ of $CP^2$ . Thus $CP^2$ does not seem to exhibit any Coulomb phase similar to U(1) but is rather more like its confining phase only.

## III Static Potentials

In order to study further the various phases of the model and in particular to compare the U(1) and CP axis we measure by Monte Carlo simulation also on an 8 x3 lattice the potential between static charges in these various regions. We follow here the method of De Grand and Toussaint (15). We do so by studying Wilson loops W(r,t) which should be very long in the t direction and are of length r in the spatial direction. For, one then has:

$$V(\vec{r}) = \lim_{t\to\infty} \frac{-1}{t} \ln(W(\vec{r},t)) \tag{7}$$

**Where $t = N_t \times$ Lattice Spacing**

Because we use periodic boundary conditions we are effectively measuring

$$W(|\vec{x}-\vec{y}|,t) = \left\langle \cos\left(\sum_1^{N_t} \Theta(\vec{x},t_i) - \sum_1^{N_t} \Theta(\vec{Y},t_i)\right)\right\rangle \tag{8}$$

The proper identification of V(r) as in eq. 8 above requires the lattice to be at finite real temperature (15). This is simulated here by taking fewer lattice points in the time direction than in the space direction. Hence the choice of $8^3 \times 3$ lattice.

In order to improve convergence we measure W only at values of $\beta_1$ and or $\beta_2$ very close to the phase transition points and average over all lengths $|\vec{x}-\vec{y}|$ ; thus we do not test for rotational symmetry of the potential.

Along the U(1) axis results for V(r) have been obtained before (15) for a Villain type action. We repeat here the calculation for the Wilson action and get similar results as shown in Fig.3. In the Coulomb phase the calculation was done using an $8^3 \times 4$ lattice at $\beta_1$ =1.10. As in reference (15) an inverse r dependence is evident. In the confining phase an $8^3 \times 3$ lattice was used ,as every where else, and at $\beta_1$ =0.97 this behavior is replaced by a predominantly linear behavior again as in Ref(15).

On the $CP^2$ axis the results we have are new. These are shown in Fig.3. Finally the potential at a point given by $\beta_1 = 1$ ,$\beta_2$ =0.6 in the Higgs phase has also been measured for the first time and is shown in Fig.4. There is clear similarity between the results in Fig.4 and those in Fig.3b and one is lead to confirm the result already evident from the phase diagram of Fig.1 namely that the low coupling (high $\beta_2$) phase of $CP^2$ is a continuation of the Higgs phase. Thus $CP^2$ does not generate here a "Coulomb" type potential as U(1) does. The similarity between the results of Fig.3a and the confining phase of U(1) in Fig.2a is harder to discern, if at all, and in fact, except for the scale, the small $\beta_2$ phase of $CP^2$ shows flat behavior with distance, similar to its other phase. It does not seem to show the linear rise characteristic of the confining U(1) phase. Note that all distances are of course in units of lattice spacing; further since the lattice is periodic over 8 units one can use the results only up to around 5 units.

## IV Discussion snd Conclusions

We have mapped out the phase diagram of a model that interpolates between $CP^2$, U(1) and O(6) models on the lattice. We immediately find that the pure $CP^2$ model has a phase transition and that its weak coupling (high $\beta_2$) phase is separated from the corresponding (Coulomb) phase of U(1). On the other hand the strong coupling phase (small $\beta_2$) appears to be in the same region as the confining phase of U(1). The shape of the phase boundaries also confirm simple arguments based on the strong coupling expansion of $CP^{N-1}$ that $CP^2$ and U(1) are expected to exhibit similar behavior in this phase and that they share similar relevant operators. However when we measure the static potential between external sources in the confining phase of U(1) we find a clear signal for linear confining potential ; on the contrary $CP^2$ does not generate such a potential in its corresponding phase. $CP^2$ with its flat potential in both of its phases generates short range forces that are similar to those from the Higgs phase potential which we also measured. Thus if dynamical generation of a gauge interaction is taking place it can only be seen in a Higgs phase where all "gauge particles" are massive.

As discussed in the introduction, hope has been expressed ( 5 ) that $CP^{N-1}$ models may generate massless composite gauge particles in the continuum. In the case discussed above this would translate ,on the lattice , to the expectation that Coulomb or confining gauge potentials similar to those of U(1) would be generated by $CP^2$ . Our main result is that this hope is not well founded. Possible modification of this result could occur if one considers larger values of N in $CP^{N-1}$ . However this would take us out of the scope of this investigation.

## Acknowledgement

K.M.B. wishes to thank C. Quigg , W.A.Bardeen and the Fermilab Theory group for their generous hospitality.

References

1. H.Eichenherr Nucl. Phys. B146,215(1978)
   A. d'Adda,M Luscher and P. DiVecchia Nucl. Phys. B146,63(1978)
2. R.D.Pisarski Phys. Rev.D 20,3358(1979)
   E. Gava, R. Jengo and C. Omero Nucl.Phys. B158,381 (1979)
   E. Brezin, S. Hikami and J. Zinn-justin Nucl. Phys. B165,528(1980)
3. E. Witten Nucl. Phys. B149,285(1979)
4. E. Cremmer and J. Scherk Phys. Lett. 74B,341(1978)
5. E. Cremmer and B. Julia Phys. Lett. 80B,48(1978)
   J. Ellis, M. K. Gaillard,and B Zumino Phys. Lett.94B,343(1980)
   and subsequent papers.
6. S. Hikami Prog. of Theo. Phys. 62,226(1979) and Kyoto Univ.
   preprint RIFP-392 (April 1980).
7. K. Wilson Phys. Rev. D14,2455(1974).
8. P. DiVecchia, A. Holtkamp,R.Musto,F. Nicodemi and R. Pettorino
   Nucl. Phys. B190(FS3)719 (1981)
   S. Duane and M. B. Green, Phys. Lett. 103B, 359 (1981).
   M. Stone Nucl. Phys. B152, 97(1979)
9. J. Frohlich, B. Simon and T. Spencer Comm. of Math. Phys. 50.
   79 (1976).
   B. Simon J. of Stat. Phys. 20,491 (1980).
10. For an alternate demonstration see M. Stone ibid.
11. B. Lautrup and M. Nauenberg Phys. Lett. 95B,63(1980).
   K.M. Bitar, S. Gottlieb and C. Zachos Phys. Lett.
   Fermilab preprint 82/56 THY.
   G. Bhanot Phys. Rev. D24,461(1981), see also ref. 12 below.
12. S. Duane and M.B. Green ibid.
13. E. Fradkin and S. Shenker Phys. Rev. D19,3682(1979)
   R. C. Brower , D.A. Kessler, T. Schalk, H. Levine and M. Nauenberg
   Nucl. Phys. B205,77 (1982)
14. When this work was done we became aware of a similar study of
   the phase diagram by S. Duane, R. Gibson and L. McCrossen
   Phys. Lett.116B, 44 (1982).
15. T. A. DeGrand and D. Toussaint Phys. Rev. D24, 466 (1981). See
   also C. B. Lang and C. Rebbi Phys. Lett. 115B, 137 (1982).

Figure Captions.

Fig.1 $CP^2$ -U(1)-O(6) phase diagram.
The dotted line is drawn to guide the eye.

Fig.2a Potential vs. distance for the confining phase of U(1) at $\beta_1 = 0.97$, $\beta_2 = 0.0$

Fig.2b Potential vs. distance for the Coulomb phase of U(1) at $\beta_1 = 1.1$ , $\beta_2 = 0.0$

Fig.3a Potential vs. distance for the $CP^2$ model at $\beta_2 = 0.725$ and $\beta_1 = 0.0$; below the phase transition point

Fig.3b Potential vs. distance for the $CP^2$ model at $\beta_2 = 0.95$ and $\beta_1 = 0.0$ ; above the phase transition point.

Fig.4 Potential vs. length in the abelian Higgs phase ; $\beta_1 = 1.0$, $\beta_2 = 0.6$

Fig.5a Hysteresis curve showing phase transition at $\beta_1 = 0.5$ and $\beta_2 = \; = 0.66 \pm .03$ with the average plaquette energy as the order parameter.

Fig.5b Hysteresis curve showing phase transition at $\beta_1 = 0.5$ ,and $\beta_2 = 0.62 \pm 0.03$ with the average energy per link as the order parameter.

Fig.6a Difference of hysteresis curves of Fig 5a.

Fig.6b Difference of hysteresis curves of Fig 5b.

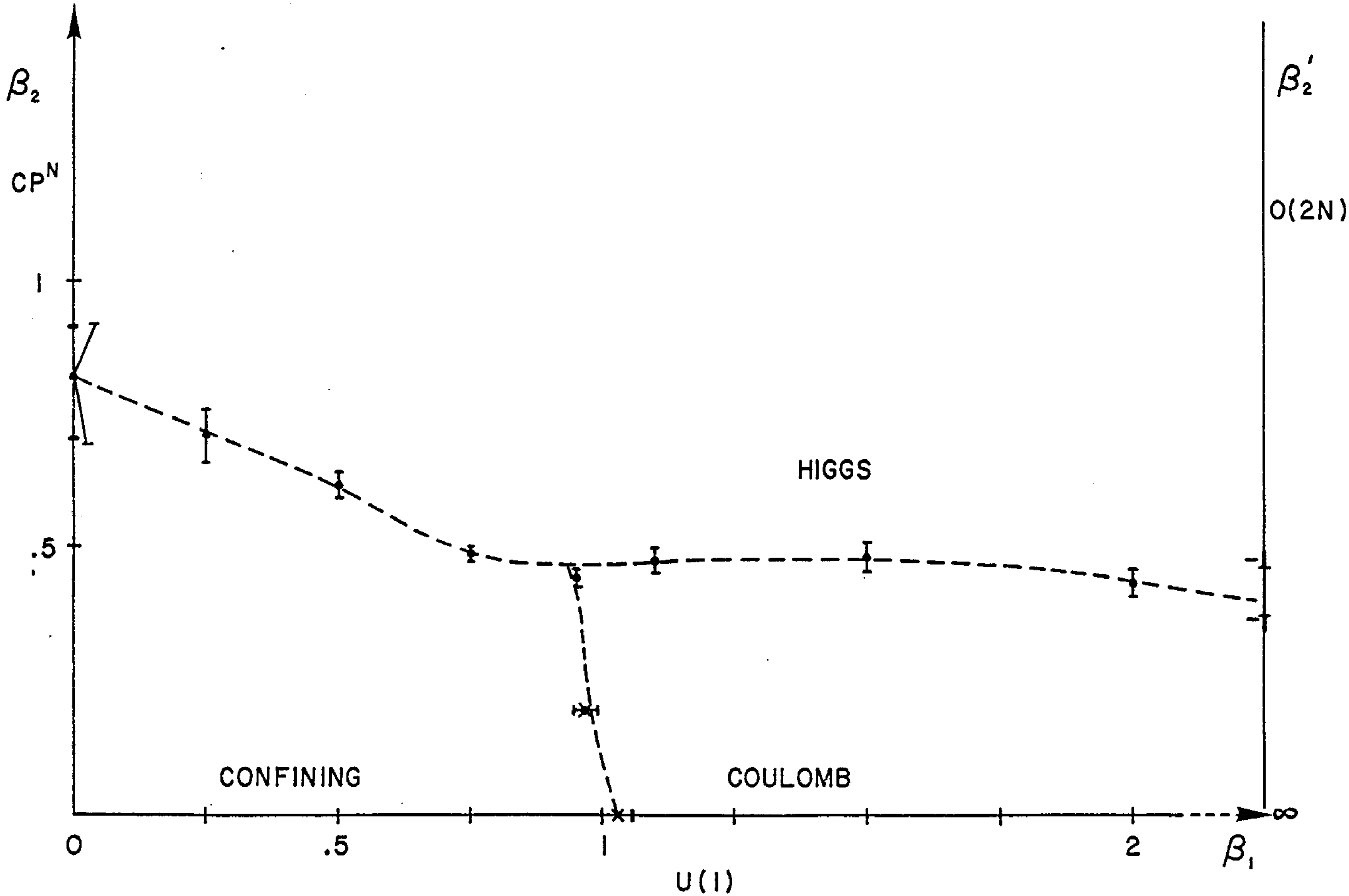


$CP^N$ - U(1) - O(2N) PHASE DIAGRAM

FIG. 1

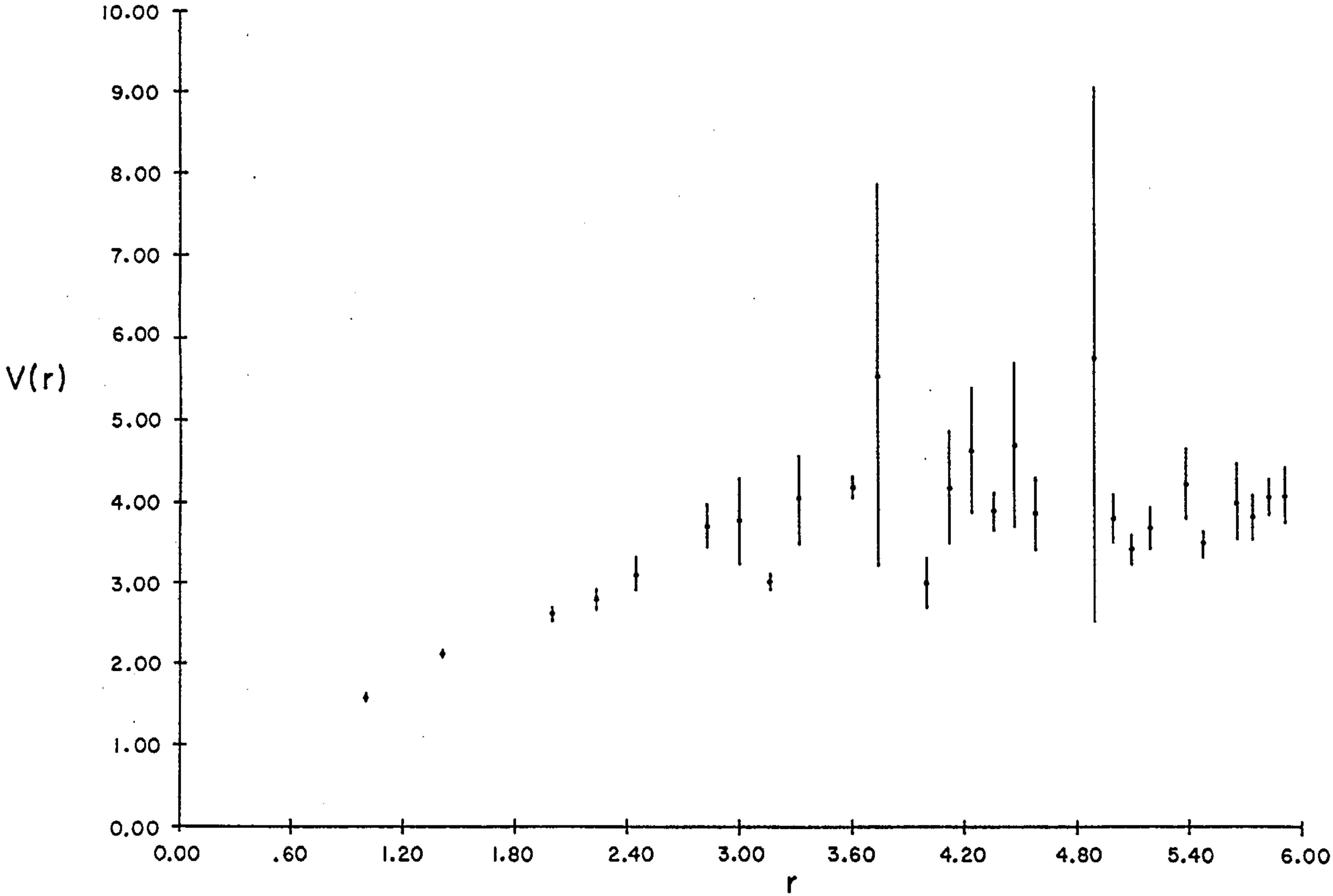
10.00
9.00
8.00
7.00
6.00
V(r)
5.00
4.00
3.00
2.00
1.00
0.00
0.00
.60
1.20
1.80
2.40
3.00
3.60
4.20
4.80
5.40
6.00
r

FIG. 2a

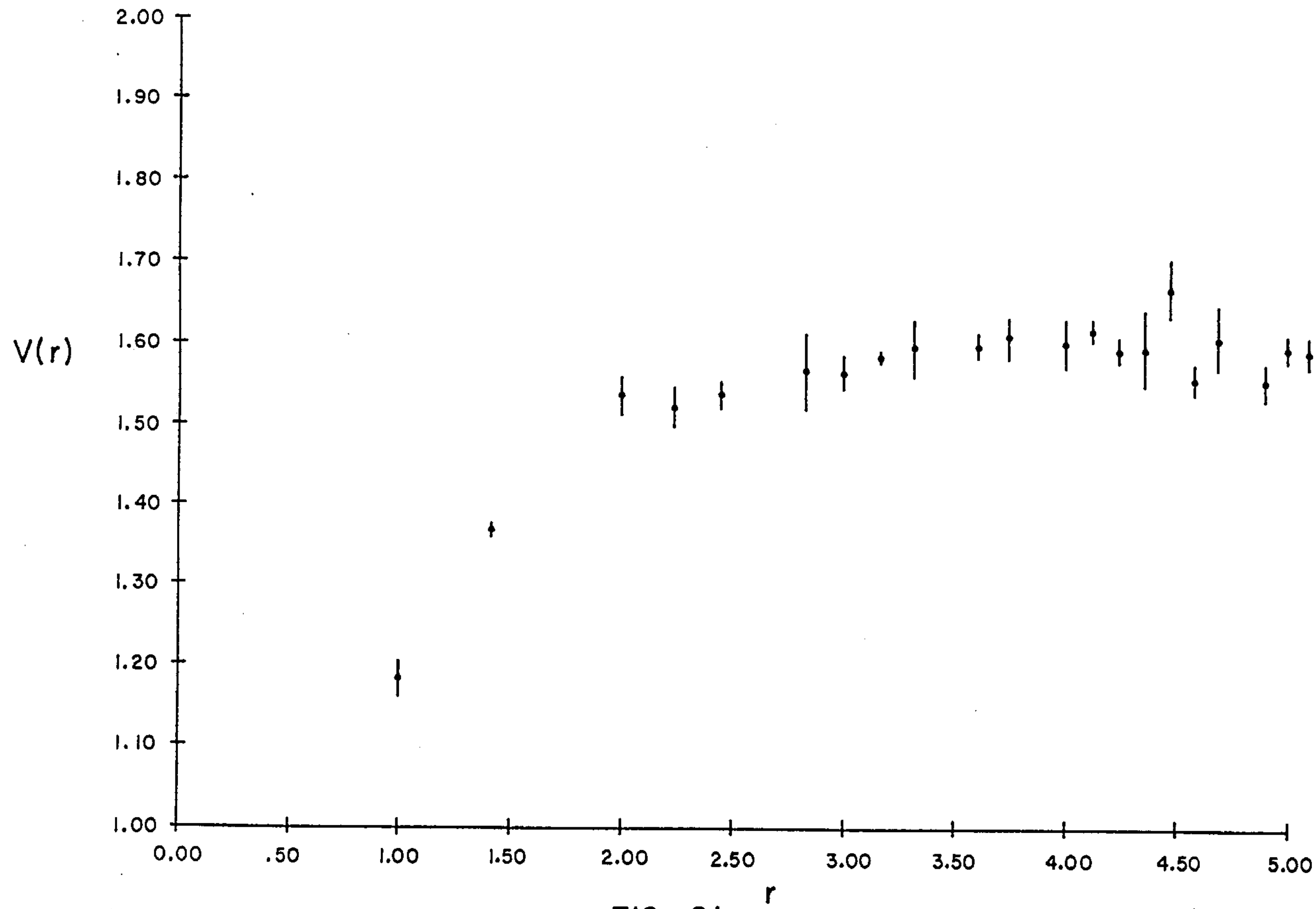
V(r)
2.00
1.90
1.80
1.70
1.60
1.50
1.40
1.30
1.20
1.10
1.00
0.00
.50
1.00
1.50
2.00
2.50
3.00
3.50
4.00
4.50
5.00
r
FIG. 2b

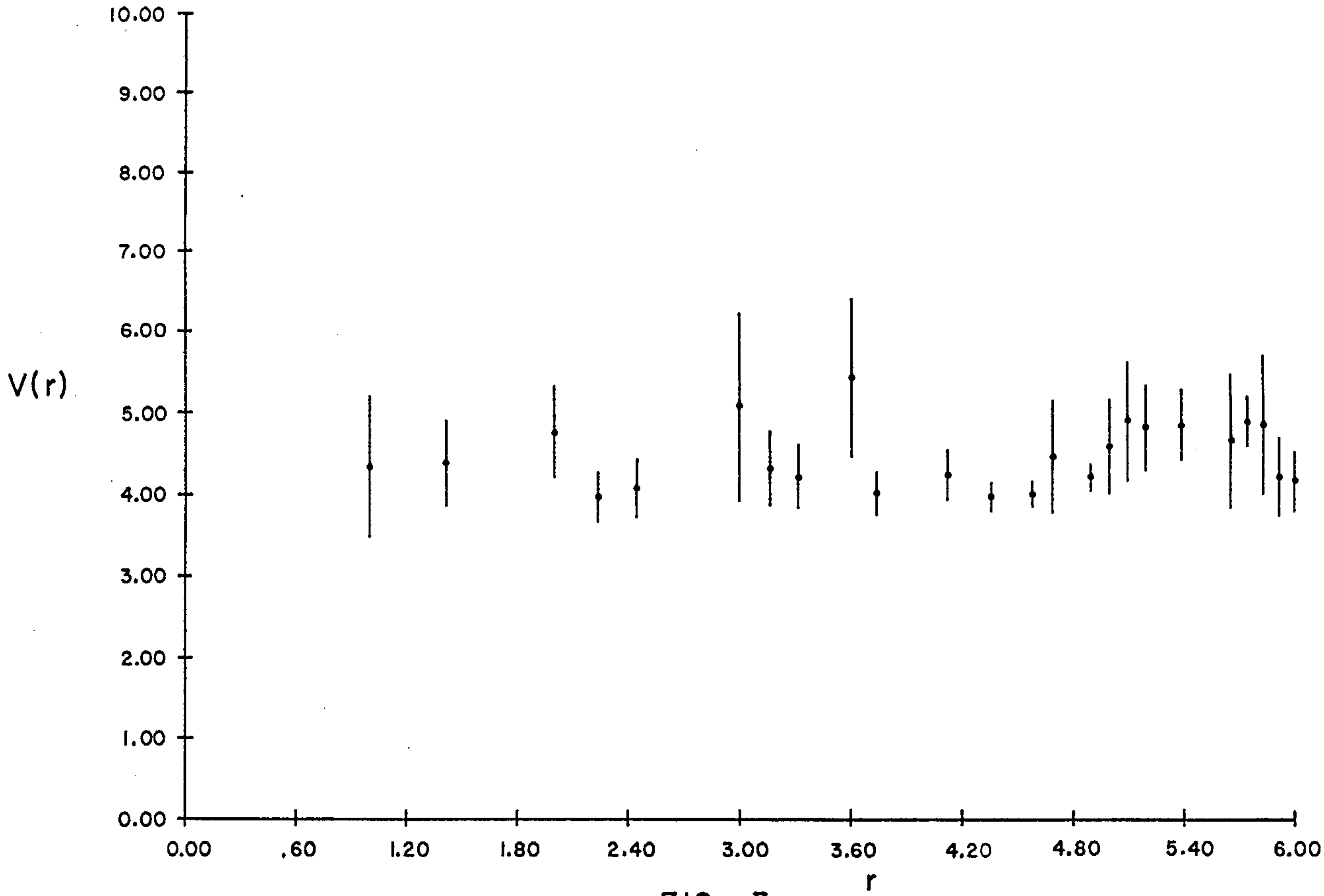
V(r)
10.00
9.00
8.00
7.00
6.00
5.00
4.00
3.00
2.00
1.00
0.00
0.00
.60
1.20
1.80
2.40
3.00
3.60
4.20
4.80
5.40
6.00
r

FIG. 3a

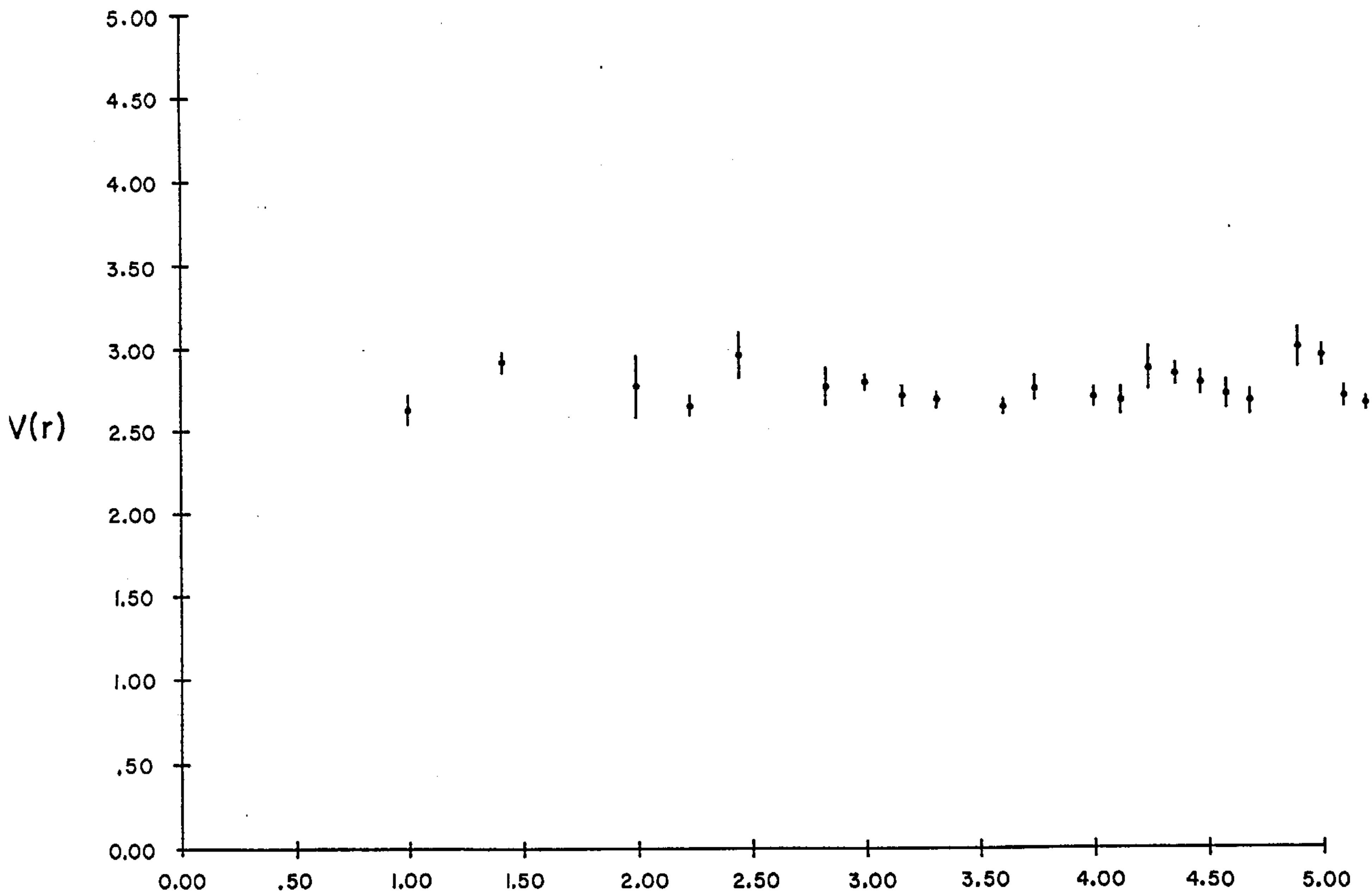
V(r)
5.00
4.50
4.00
3.50
3.00
2.50
2.00
1.50
1.00
.50
0.00
.50
1.00
1.50
2.00
2.50
3.00
3.50
4.00
4.50
5.00

r

FIG. 3b

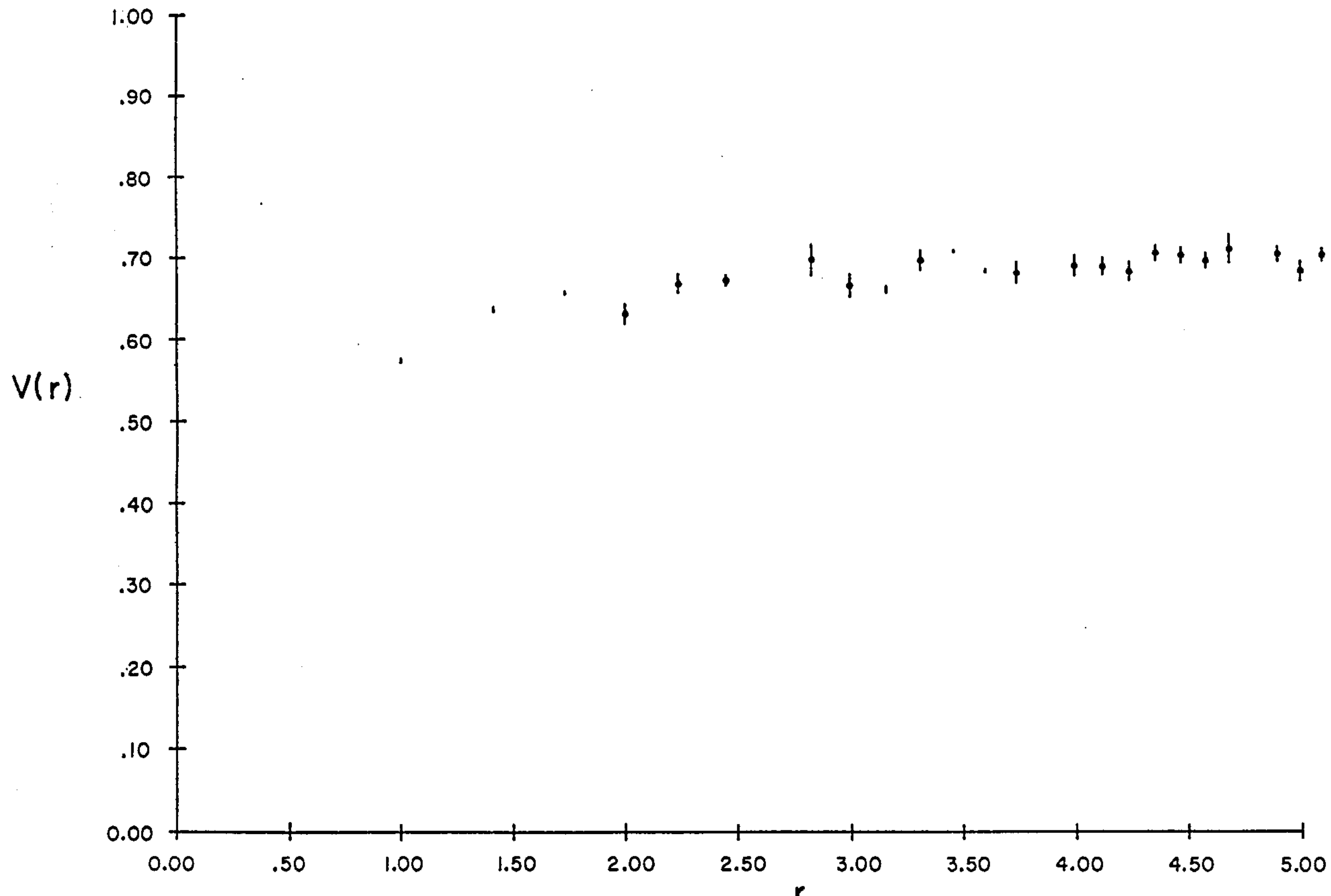

1.00
.90
.80
.70
.60
V(r)
.50
.40
.30
.20
.10
0.00
0.00
.50
1.00
1.50
2.00
2.50
3.00
3.50
4.00
4.50
5.00
r


FIG. 4

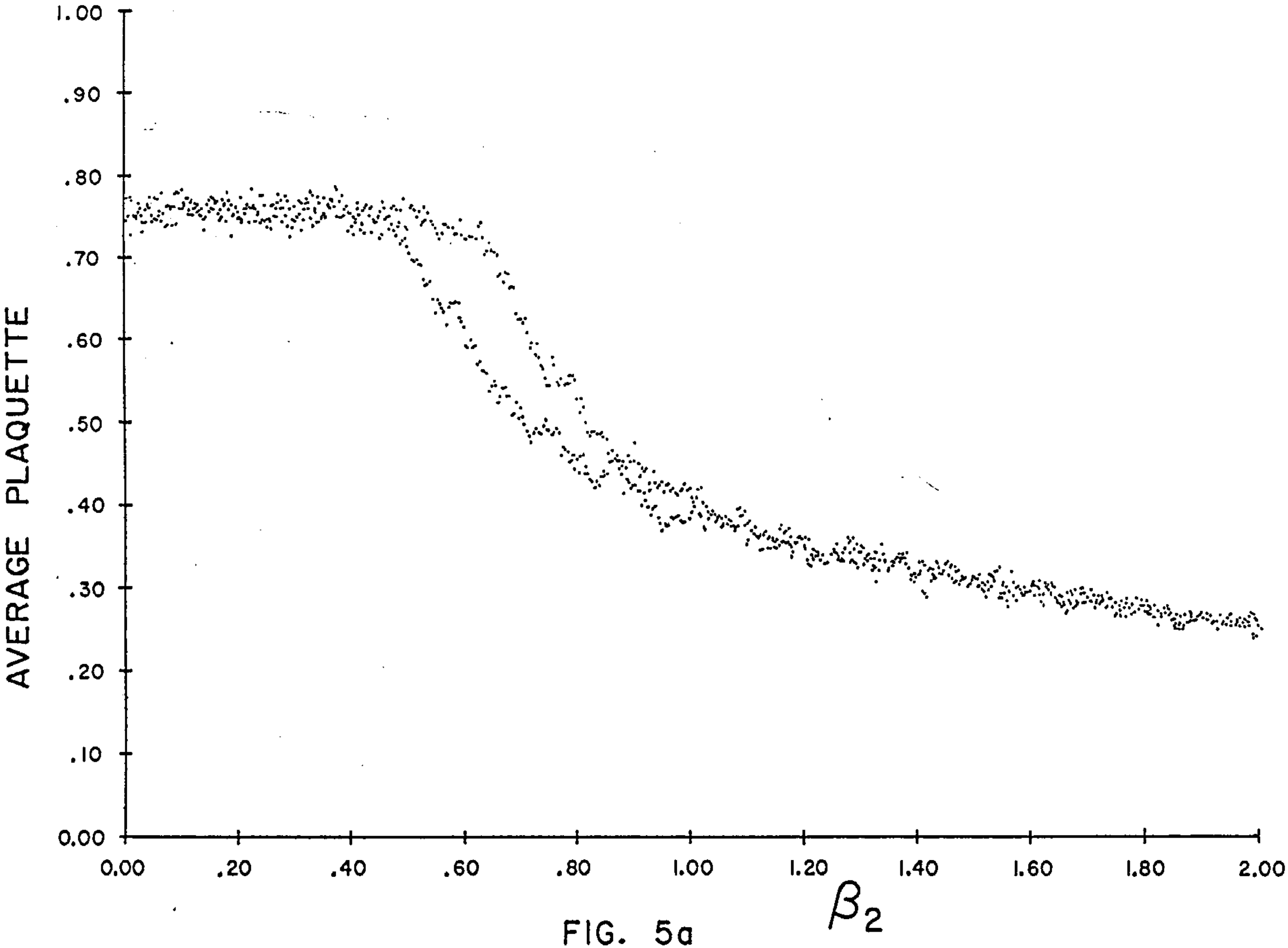
AVERAGE PLAQUETTE
1.00
.90
.80
.70
.60
.50
.40
.30
.20
.10
0.00
0.00
.20
.40
.60
.80
1.00
1.20
1.40
1.60
1.80
2.00
$\beta_2$

FIG. 5a

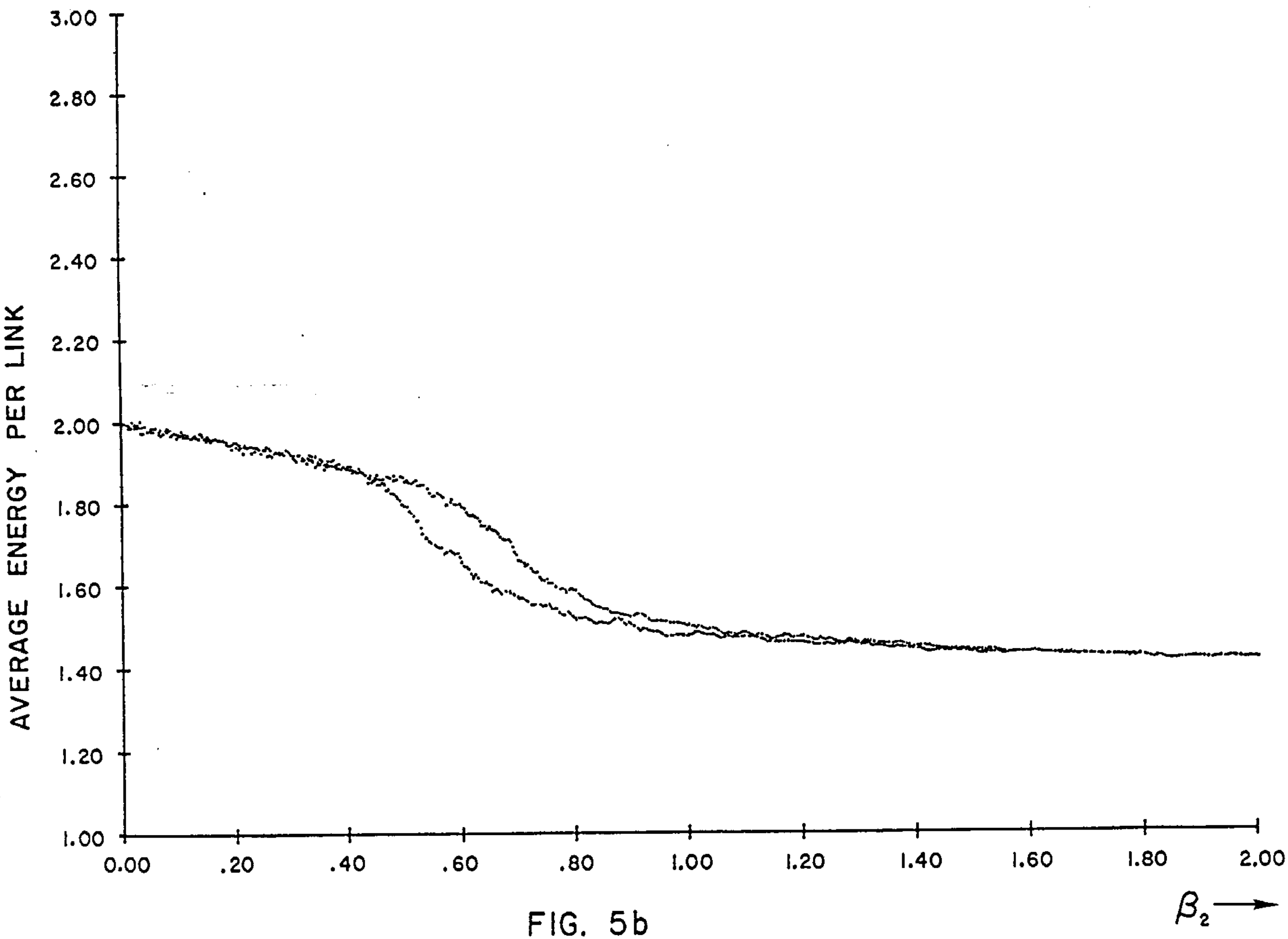
AVERAGE ENERGY PER LINK
3.00
2.80
2.60
2.40
2.20
2.00
1.80
1.60
1.40
1.20
1.00
0.00
.20
.40
.60
.80
1.00
1.20
1.40
1.60
1.80
2.00
$\beta_2$

FIG. 5b

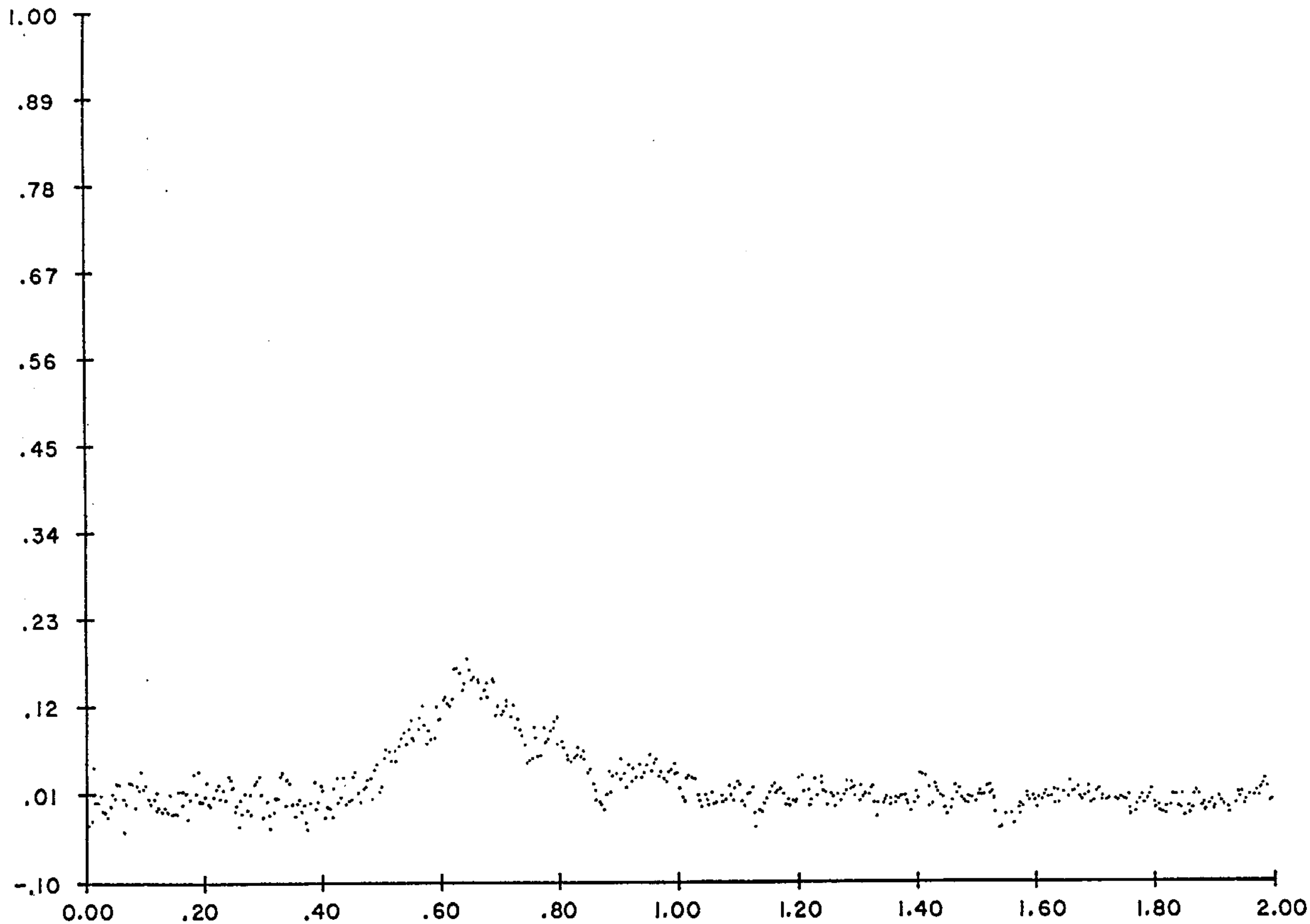
1.00
.89
.78
.67
.56
.45
.34
.23
.12
.01
-.10
0.00
.20
.40
.60
.80
1.00
1.20
1.40
1.60
1.80
2.00

FIG. 6a

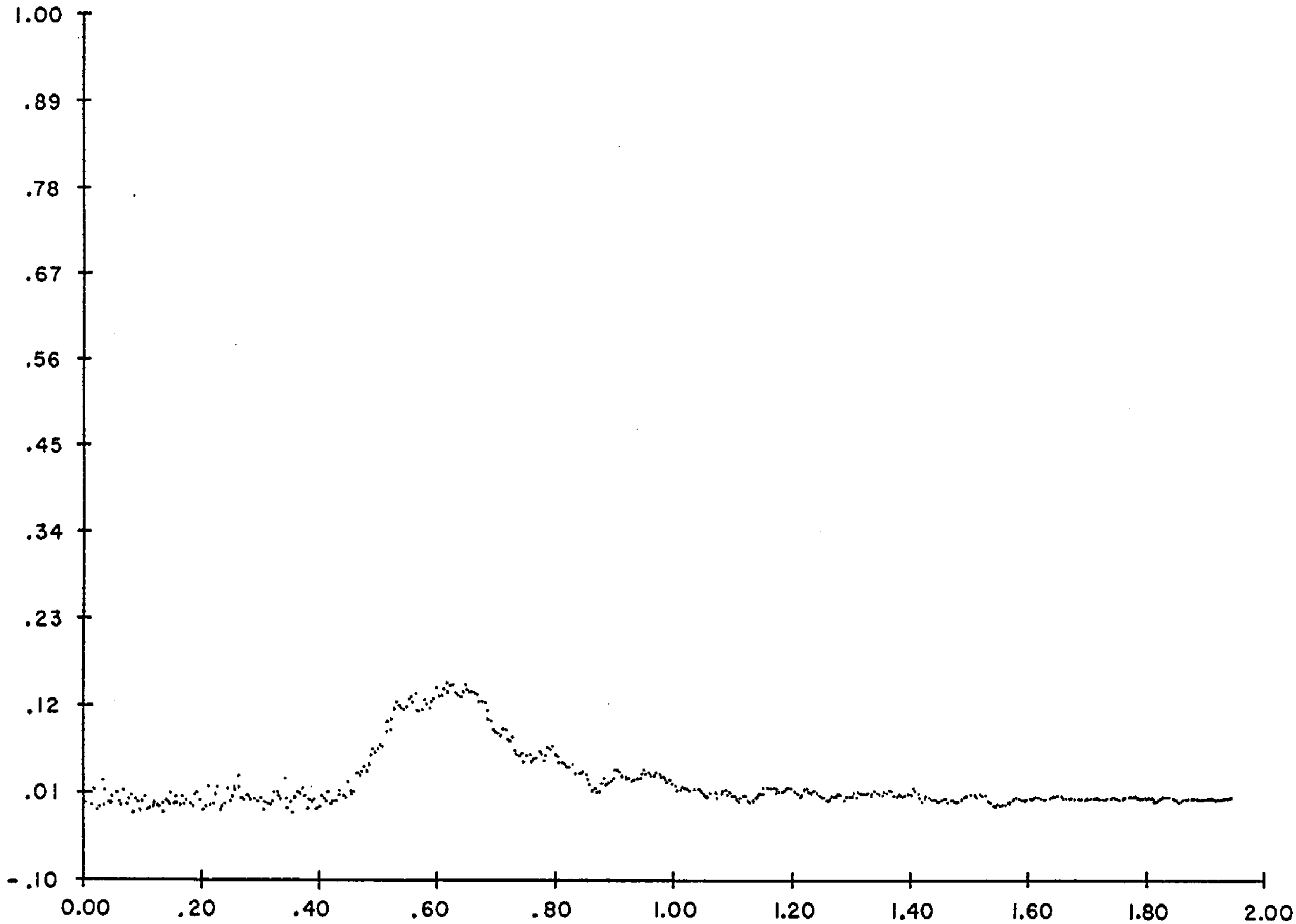
1.00
.89
.78
.67
.56
.45
.34
.23
.12
.01
-.10
0.00
.20
.40
.60
.80
1.00
1.20
1.40
1.60
1.80
2.00

FIG. 6b